Leszek ROMAŃSKI
Jerzy BIENIEK
Piotr KOMARNICKI
Marcin DĘBOWSKI
Jerzy DETYNA

OPERATIONAL TESTS OF A DUAL-ROTOR MINI WIND TURBINE

BADANIA EKSPLOATACYJNE DWUWIRNIKOWEJ MINI ELEKTROWNI WIATROWEJ*

The article presents the results of wind-tunnel tests and field studies of a mini dual-rotor wind turbine. The first stage involved testing of an open-circuit wind tunnel built with the aim of performing laboratory tests. The coefficient of uneven air stream distribution at a rated speed was 1.7%, while the index of turbulence intensity in the entire measurement range was between 1.2 and 1.8%. The mini wind turbine was equipped with rotors with new design blades. Compared to the blade designs used in mini wind turbines available on the market, the blades used in the present study were characterized by an efficiency of 0.28. The results of performance tests in the wind tunnel were evaluated statistically using Pearson correlation coefficients and Spearman's rank. We examined the relationship between a dependent variable (power P) and independent variables (average air stream speed V, incidence angle of the blades of the first rotor α_1, incidence angle of the blades of the second rotor α_2, and the distance between the rotors l). The analysis showed, as expected, that the strongest correlation was between power and speed of the air stream. While incidence angles of the two rotors also affected the turbine's power, no such effect was observed for changes in the distance between the rotors. Field tests confirmed the findings and observations made in the wind tunnel.

Keywords: *operation, mini dual-rotor wind turbine, wind tunnel.*

W artykule przedstawiono wyniki badań dwuwirnikowej mini elektrowni wiatrowej przeprowadzone w tunelu aerodynamicznym oraz w terenie. W pierwszym etapie testowano zbudowany w celu przeprowadzenia badań laboratoryjnych tunel aerodynamiczny o konstrukcji otwartej. Wyznaczony współczynnik nierównomierności strugi powietrza przy prędkości nominalnej wynosił 1,7%, natomiast wskaźnik intensywności turbulencji w całym zakresie pomiarowym zawierał się w granicach 1,2-1,8%. Budując mini elektrownię wiatrową wyposażono ją w wirniki w których zastosowano nową konstrukcję łopat. Zastosowane łopaty w porównaniu do zbliżonej konstrukcji łopat stosowanych w mini elektrowniach dostępnych na rynku charakteryzowały się sprawnością wynoszącą 0,28. Po wykonanych badaniach eksploatacyjnych w tunelu aerodynamicznym uzyskane wyniki poddano ocenie statystycznej z wykorzystaniem współczynników korelacji liniowej Pearsona oraz rangi Spearmana. Zbadano zależności między zmienną zależną (moc P) oraz zmiennymi niezależnymi (średnie prędkości strugi powietrza V, kąt zaklinowania łopat pierwszego wirnika α_1, kąt zaklinowania łopat drugiego wirnika α_2, odległości pomiędzy wirnikami l). Na podstawie analizy, zgodnie z oczekiwaniem, stwierdzono, że najsilniejsza korelacja występuje w odniesieniu do prędkości strugi powietrza. Wpływ na moc mają także kąty zaklinowania na obu wirnikach, natomiast nie stwierdzono takiego wpływu w przypadku zmian odległości pomiędzy wirnikami turbiny. Badania w terenie potwierdziły ustalenia i spostrzeżenia poczynione w tunelu aerodynamicznym.

Słowa kluczowe: *eksploatacja, mini elektrownia wiatrowa dwuśmigłowa, tunel aerodynamiczny.*

1. Introduction and objectives

According to the formula for power generated by wind turbines, the speed of the incoming air stream working on the turbine rotor (speed in the third power) and the diameter of the rotor itself (second power) have the greatest impact on power. In the first case, excluding a situation when the wind turbine is running in a diffuser, we are entirely dependent on the forces of nature, because we have virtually no effect on wind power. In the second case, it seems that all simple solutions have already been exhausted, because enlarging the diameter of rotors above 140 m is connected with great technological problems and a very large, disproportionate increase in manufacturing costs [19]. A cheaper option, which additionally affects the efficiency of the turbine, is to improve the design of the blades themselves. Their geometry and size have to be changed in such a way as to generate on them an increasing lift force during the rotation of the rotor at the same wind speed [3, 10, 16, 26].

Recently many designers have been working on the problem of additional uses of the energy of the air stream when it is already out of

the wind turbine rotor in its post-action phase. An example of a design in which this "waste energy" can be utilized is a wind turbine with two rotors situated in the axis of the electric generator [18, 21, 22, 23, 24]. There are two versions of this solution (Figure 1).

In the first design (Fig. 1a), the assembly has two rotors rotating in the same direction. Shaft speed is increased by the use of transmissions. As the electrical generator is propelled by two rotors, the efficiency of the generator increases, which is especially observable in low wind conditions.

In this arrangement, the turbine may also work in the counter-rotating mode, which increases the efficiency of the assembly. The second concept features a structure (Fig. 1b) with two rotors positioned axially before the generator. Rotor assemblies intercept air mass flowing from one direction. The structure of the wind turbine is gearless and the individual components of the generator (stator, rotor) are driven by different turbines. Under the action of flowing air mass, the rotors with different blade pitch rotate in opposite directions. Consequently, the relative rotation speed of the rotor is greater than in
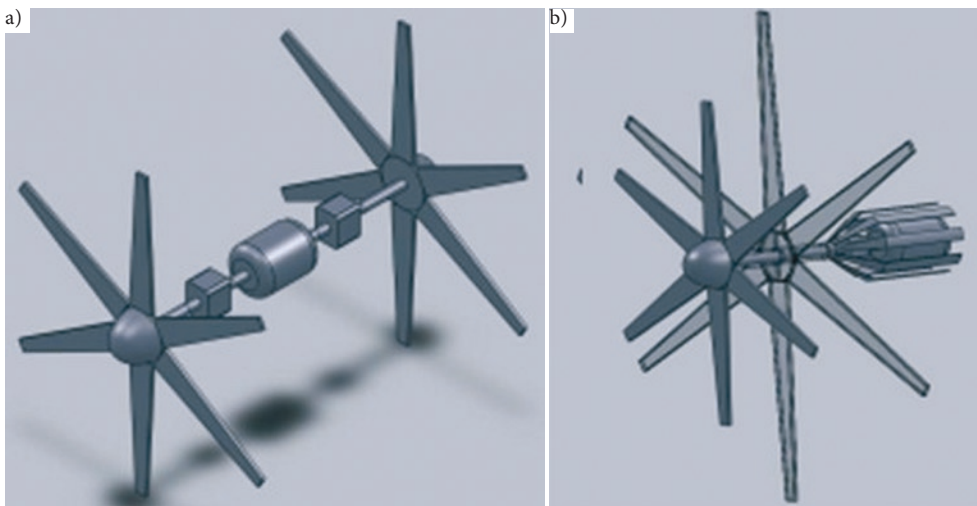
Fig. 1. The relative position of two rotors in wind turbines: a – rotors situated on both sides of the generator, b – rotors situated axially one behind the other [17]

2. Material and method

In the present study, a wind tunnel was used as the basic test stand for evaluating the performance of different aerodynamic objects, including mini wind turbines. The tunnel was designed and built on the basis of information available in the literature [4, 5, 7, 8, 9] and counsel provided by specialists in the field from several research centres. The shape of the Witoszyński confusor used in constructing the tunnel was determined numerically [1, 6, 11]. The combined use of a stream straightener and the Witoszyński confusor yielded an increase in air velocity in the measuring chamber, giving a more concentrated and steady flow. The basic geometric dimensions of the tunnel were as follows: square inlet 2.5 x 2.5m large,

single-rotor structures. As a result, the power generated by the turbine should increase.

Among other solutions, axial flux permanent magnet generators, also known as low-speed generators, are used in the construction of low-power wind turbines. Their use makes it possible to eliminate or reduce the mechanical transmission ratio. This reduces noise and costs of the assembly and increases its efficiency. Low-speed generators are made as cylindrical or disc generators. An example of an axial flux generator with a coreless stator is shown in Figure 2. It has a relatively simple structure; since there is no loss in the stator core, its efficiency is increased [13, 14].

Based on the literature and the authors' experience, a dual-rotor mini wind turbine was designed and built, in which one rotor drove the propeller and the other one drove the stator of the generator in the opposite direction. Operational tests were carried out in the wind tunnel and in natural conditions in the foothill region of the Sudetes.
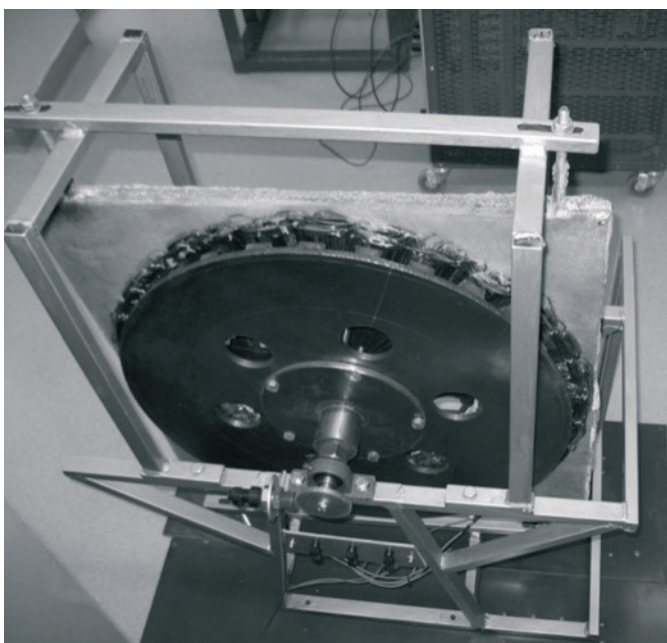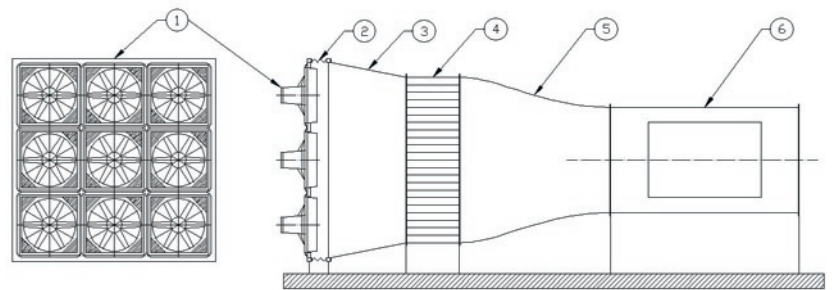

Fig. 3. Diagram of an open circuit wind tunnel: 1 – frame with fan section, 2 – vibration damper, 3 – square-section symmetrical contraction, 4 – honeycomb screen, 5 – the Witoszyński confusor, 6 – test chamber with an observation window [15]

total length 7m, and outlet – a measurement chamber with a diameter of 1.4 m (Fig. 3). The use of nine independently controlled axial fans, 2.2 kW power units, made it possible to achieve an air stream velocity in the measuring space of up to 17.5 m·s^{-1} at a dynamic pressure of approximately 200 Pa and to obtain a balanced stream velocity gradient in the cross-section of the measuring chamber. The fans were controlled through changes in the rotational speed of the rotors made by adjusting the frequency of power inverters in the range of 15–50Hz in 0.01 Hz increments [15].

The wind tunnel was tested when the test chamber was empty. Air flow testing in the tunnel was performed in two stages. In the first stage, the basic parameters of the stream were determined including pressure, velocity and qualitative indices of the tunnel such as the uniformity of velocity distribution in the test chamber and turbulence intensity indicators, which were considered as a function of the arithmetic mean of velocity. In the second stage, we investigated the effect of adjusting the operation of the individual fans on the distribution of velocity fields in the test section of the wind tunnel. Measurements of uniformity of stream velocity distribution in the test chamber were done using the traversing method according to the Polish standard PN-ISO 5221. The measurement points were arranged in the circular cross-section measuring channel on the basis of the Log-Chebyshev method recommended in the standard. In accordance with the aforementioned method, the channel was divided into concentric rings. Because the channel had a diameter greater than 0.25m, it was divided into five rings. The centre of the channel was measured in relation to
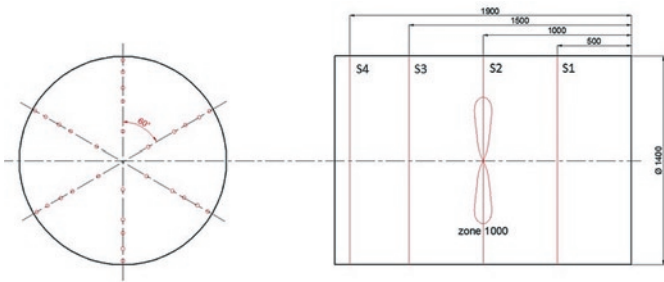

Fig. 2. A model of a low-speed axial flux generator [14]

Fig. 4. *Schematic layout of measurement points when traversing the cross section of the channel and the location of the measurement zones over the entire length of the chamber [15]*

the axis of symmetry of the duct. In order to obtain a proper mean, an equal number of measurements was performed on each of the rings. 10 measurement points were located on 3 axes inclined with respect to each other at an angle of 60° (Fig. 4). Tests of the field distribution of flow rate were performed in 4 selected measurement areas: S1, S2, S3, and S4, whose distance from the edge of the outlet was 0.5, 1.0, 1.5, and 1.9 m, respectively [15].
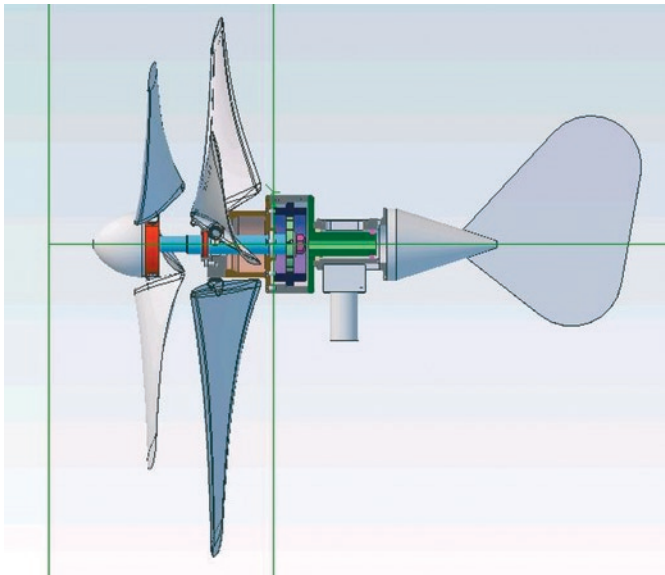

Fig. 5. *Schematic diagram of the dual-rotor wind turbine built at the Institute of Agricultural Engineering of the Wrocław University of Environmental and Life Sciences*

A diagram of the tested dual-rotor turbine is shown in Fig. 5. The functional model of the turbine was designed for quick installation of different shapes of blades, setting of their angle of attack and changing the position of the rear rotor relative to the front rotor. The incidence angle of the first blade (parameter α_1) could take six values between 125° and 150° in 5° increments. The incidence angle of the second blade (parameter α_2) could also take six values between 30° and 55° in 5° increments. The distance between the rotors was adjusted from 0.105 m to 0.14 m, in 5 mm increments.

As part of the research, new types of wind turbine blades were designed and built, which proved to be highly efficient aerodynamically. Appropriate airfoils of the blades were designed after a comparative analysis of numerous different shapes discussed in the literature [2, 12, 20, 23, 25], development of numerical models, and the authors' model-based tests. The blades were made using CNC technology and built with several layers of material, i.e., epoxy-glass composite, and their structures were based on two efficient aerodynamic airfoils.
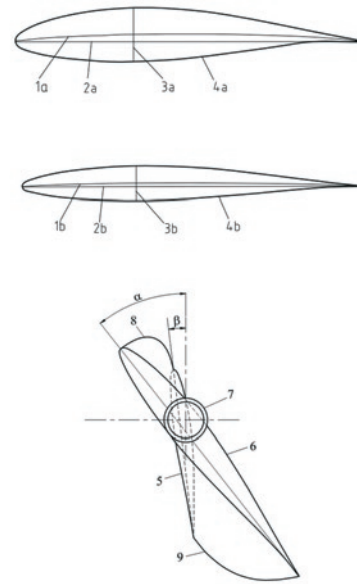

Fig. 6. *The outlines of the initial airfoil NACA 63-415 and the end airfoil NACA 63-210 and view from the blade's mounting root: α - incidence angle of the initial airfoil, β - incidence angle of the end airfoil, 1a, 1b - camber line, 2a, 2b - chord line, 3a, 3b - airfoil thickness, 4a, 4b - airfoil curve, 5 - plane of the end airfoil NACA 63-210, 6 - plane of the initial airfoil NACA 63-415, 7 - mounting root, 8 - leading edge, 9 - trailing edge*

Figures 6 present an exemplary airfoil of a twisted blade NACA 63-415-NACA 63-210.

An important element of any wind turbine is the generator, whose task is to produce electricity as a result of rotation of the blades. The tested mini-turbine used a solution in which the rotor and the stator rotated independently in opposite directions.

It was assumed that the generator rotors would rotate in opposite directions. Figure 7 shows a model of a prototype generator constituting an integral whole of the mini-wind turbine using a synchronous permanent magnet generator.

Operational tests of the mini dual-rotor wind turbine were carried out in two stages (Figure 8): the first stage was conducted in a wind tunnel (Figure 8a) with assumed constant operating parameters and the second stage featured field conditions (Figure 8b) of the village Wiry near Sobótka. Long-term observations of the Institute of Meteorology and Water Management show that the average wind speed in the region of Lower Silesia is 3.5 m·s^{-1} and the annual wind energy
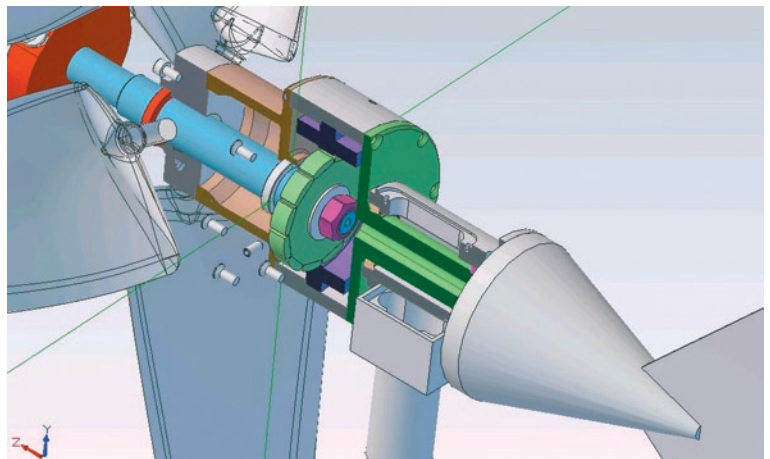

Fig. 7. *Schematic diagram of the dual-rotor wind turbine built at the Institute of Agricultural Engineering of the Wrocław University of Environmental and Life Sciences*
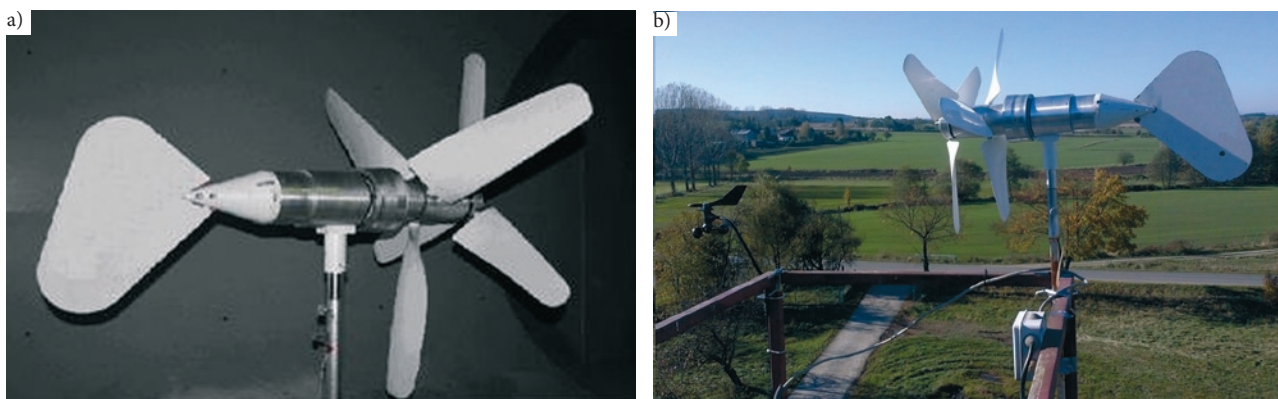
a)   b)

Fig. 8. View of the tested mini turbine in operation: a- in the wind tunnel, b- during the field tests
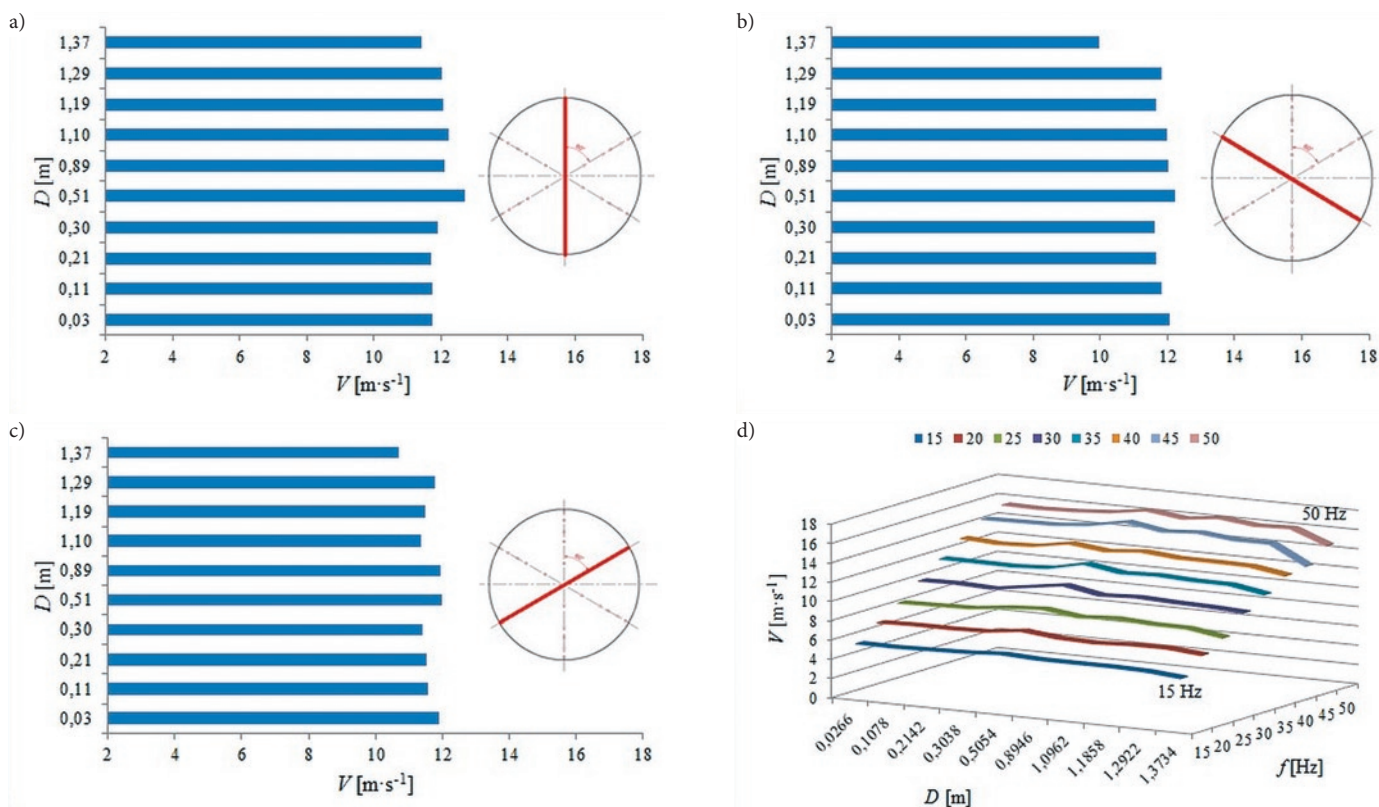
a)   b)

c)   d)

Fig. 9. Sample distributions of air stream speed in the measuring chamber for the setting of fan frequency at 35 Hz in the zone S2: a - measurements for the axis 90°, b - measurements for the axis 150°, c - measurements for the axis 210°, d - characteristics of speed distributions for the full range of fan settings
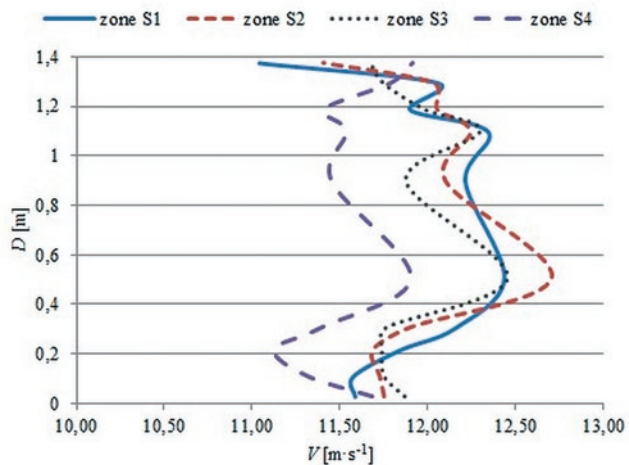

Fig. 10. Base air stream speed profiles for 4 different measurement zones for the setting of fan frequency at 35 Hz

is approx. 1,000 kWh·m^{-2}. Given the distribution of wind speeds in different months of the year, as well as wind energy conversion efficiency into electricity of approx. 20%, it was assumed that 1 m^2 of wind stream would yield only 0.53 kWh per day. The wind turbine was connected to a voltage regulator, a battery and a transmitter which collected data on the energy generated in the turbine (voltage, amperage) as well as data from a weather station installed near the wind turbine. For statistical analysis, the statistical software package Statistica v.10 by StatSoft was used.

3. Results

Due to the fact that wind turbines achieve their rated power at wind speeds of around 10-12 m · s^{-1}, the article provides an example of the air flow profiles measured in the measuring chamber corresponding to these speeds (Figure 9).
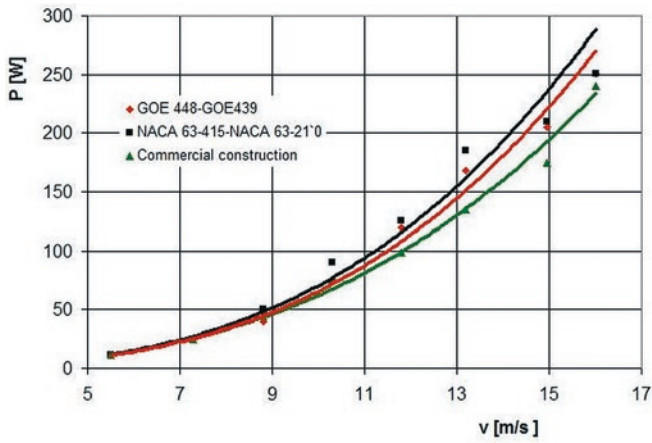
Fig .11. *Power curve of the tested mini wind turbine using various blade designs*

Table 1. *Efficiency coefficients of the tested turbines*

Turbine or airfoil name	Rotor diameter (m)	Wind power (W) at $V = 12$ m·s^{-1}	Power supplied by the rotor (W)	Efficiency reached (-)
JSW-750-12	0.75	471.4	97	0.21
GOE – 448/439	0.75	471.4	120	0.25
NACA 63-415/210	0.75	471.4	131	0.28

Table 2. *Pearson and Spearman coefficients determining the statistically significant correlation between the dependent variable and the independent variables for the dual-rotor wind turbine*

Independent variable	Pearson correlation coefficients	Spearman's rank correlation coefficient
V	0.90	0.95
α_1	−0.16	−0.14
α_2	0.17	0.13
l	0.02	0.02

The presented distributions corresponded to frequency settings of fans at 35 Hz. Based on the obtained basic distributions, it was observed that the air stream was characterized by slight irregularity and increased speed values in the vicinity of the axis of the measuring chamber.

The maximum local value of dynamic pressure was 198 Pa and was obtained by setting the frequency of the current supplying the fan motors at 50 Hz. Air stream velocity was calculated at 17.55 m·s^{-1}. Local minimum dynamic pressure values for the setting of 15 Hz amounted to 17 Pa, while the stream velocity was calculated at 5.14 m·s^{-1}. The impact of the distance of measuring areas S1-S4 on stream velocity profile is shown in Figure 10.

The designated index of turbulence intensity ranged between 1.2-1.8% [15]. The comparison of the performance of the mini wind turbine with removable rotors consisting of blades with different airfoils was based on a compilation of the plotted power characteristics.

Test results of the new design of the blades in relation to factory models are shown in Figure 11. Testing was performed in each case for 5 different incidence angles. The graph shows power curves which characterise the given blade at an "optimal" incidence angle. Both of the new designs of rotor blades proved to be more efficient than the factory rotors (Table 1).

The resulting efficiency of the mini wind turbine relative to the power of wind stream at the inlet to the rotor was 0.21 for the factory
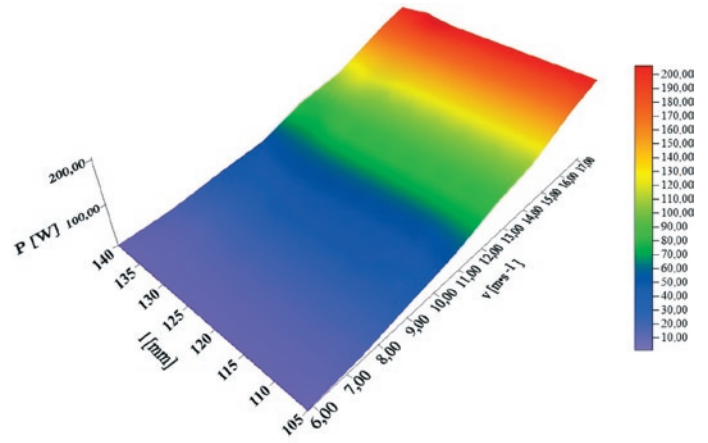

Fig. 12. *Dependence of generated power on the distance between the rotors and the average air stream velocity for blade incidence angles α1 = 125° and α2 = 50°*
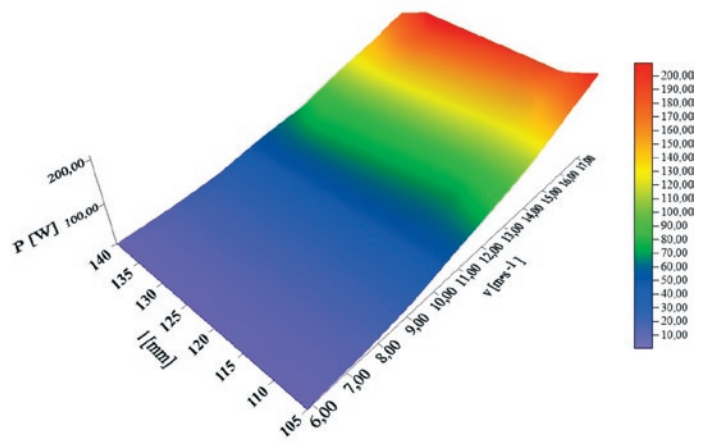

Fig. 13. *Dependence of generated power on the distance between the rotors and the average air stream velocity for blade incidence angles $\alpha_1 = 130°$ and $\alpha_2 = 55°$*
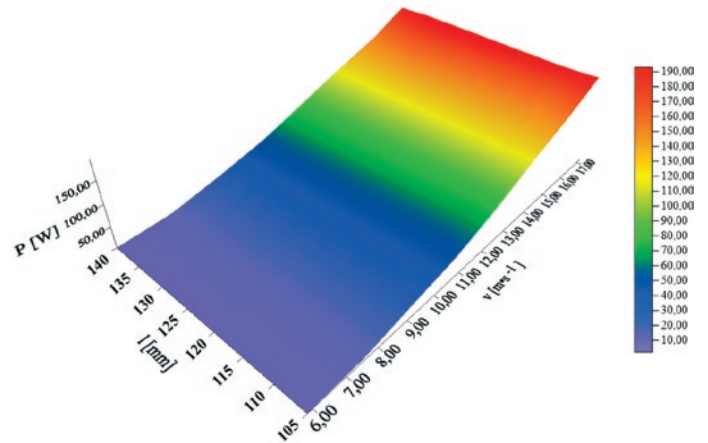

Fig. 14. *Dependence of generated power on the distance between the rotors and the average air stream velocity for blade incidence angles $\alpha_1 = 125°$ and $\alpha_2 = 40°$*

turbine with 0.25 declared in the device's manual. In the case of the wind turbine with the GOE airfoil rotor blades, it was 0.25. When comparing

the power values of all the tested rotors at 12m·s^{-1}, which is recognized as the rated wind speed, it was observed that both designs generated more electricity: 19.5% for the GOE blade airfoil and 23.7% for
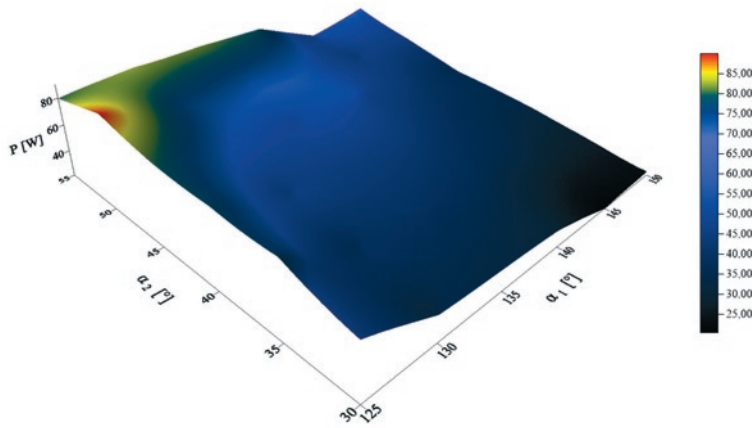
Fig. 15. Power characteristics as a function of blade incidence angles in particular rotors for the air stream velocity of 12.41m·s⁻¹

NACA, respectively. It is worth emphasizing that the new rotors have higher generated power values in the entire tested speed range. The rotor with NACA blades reached the efficiency of 0.28.

In order to obtain optimum settings of the rotors for field research, it was necessary to conduct a statistical analysis based on the results obtained in the wind tunnel tests. It was mainly aimed at determining the statistically significant relationship between the dependent variable (power P) and independent variables (average air stream velocity V, incidence angle of the blades of the first rotor α_1, incidence angle of the blades of the second rotor α_2, the distance between the rotors l) with the use of Pearson correlation coefficients and Spearman's rank. The results are shown in Table 2.

Based on the analysis, it can be concluded that the strongest correlation (in both cases coefficients ≥ 0.90) occurs for the air stream velocity, which is logical and confirmed by tests. Weak negative correlation occurs for the incidence angle of the blades of the first rotor. The negative coefficients suggest that reducing the incidence angle

should result in an increase in power generated. Also a weak but positive correlation occurs for the incidence angle of the blades of the second rotor. Positive values of coefficients describe the increase in power generated along with increasing value of the incidence angle of the blades. Statistically significant lack of correlation for the two indices occurs in relation to the distance between the rotors. The absence of such correlations is illustrated by three exemplary three-dimensional graphs shown in the figures: 12 – 14. They were made as $P = f(l; v)$ for:

$\alpha_1 = 125°$ and $\alpha_2 = 50°$; $\alpha_1 = 130°$ and $\alpha_2 = 55°$; $\alpha_1 = 125°$ and $\alpha_2 = 40°$.

The analysis of the data in these figures indicates that speed has a significant impact on the power generated by the wind turbine, as opposed to the distance between the rotors which has no such effect. Due to the compactness of the structure, this distance should be as small as possible while maintaining a safe enough distance between the rotors in the event of hurricane winds; when blades deviate from the perpendicular there can be no contact between the blades as it would result in their mutual damage. In order to determine the optimal incidence angle of the blades from the point of view of power delivered by the wind turbine, the dependencies resulting from the function $P=f(\alpha_1; \alpha_2)$ were presented in a graphic form. The figures were made for eight air stream speeds within the measuring range from 5.58 to 17.17 m·s⁻¹. Figure 15 shows an example of the stream speed graph for 12.41 m·s⁻¹. Selected optimal values of incidence angles of blades for specific values of air stream speed are summarized in Table 3.

A histogram (Fig. 16) of the sets of incidence angles makes it much easier to draw conclusions due to the fact that some of these same sets of blade incidence angles (α_1, α_2) allow the turbine to generate the most power at given air stream speeds.

After analysing the data relating to the power generated at a particular wind speed for the given incidence angles α_1 and α_2, it can be concluded that the optimal configuration values are 125° for the first rotor blades and 50° for the second rotor blades of the wind turbine. Other acceptable configurations:

$\alpha_1 = 130°$ and $\alpha_2 = 55°$; $\alpha_1 = 125°$ and $\alpha_2 = 40°$.

Table 3. Selected optimal incidence angles of blades for the air stream speed of 12.41 m·s⁻¹

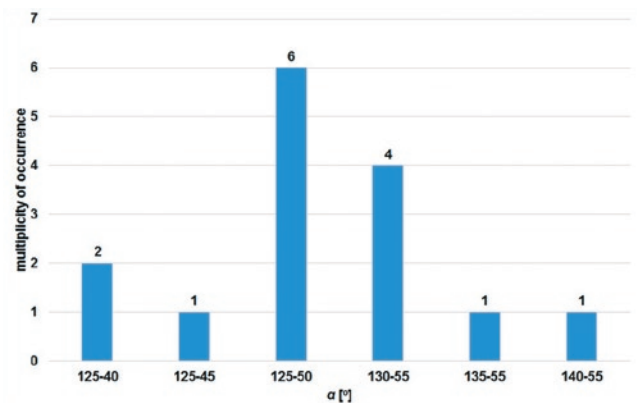| v_{avg}	α_1	α_2
m·s⁻¹	°	°
5.85	125	40
7.53	125	50
9.17	125	50
10.82	125	50
10.82	130	55
12.41	125	50
14.08	125	40
14.08	125	45
14.08	125	50
14.08	130	55
14.08	135	55
14.08	140	55
15.82	125	50
15.82	130	55
17.17	130	55

Fig. 16. The number of times a setting of incidence angles of the blades of the first and second rotor occurs after the dual-rotor wind turbine has reached its maximum power capacity for a given air stream speed

Specifications of the dual-rotor mini wind turbine are summarized in Table 4.

Figure 17 shows the results of simulations of the performance of the wind turbine in the wind tunnel under changing working conditions reflecting the conditions that occur during wind gusts. After analysing the electrical power generated by the plant it can be concluded that the moment of power capacity increase is recorded only after a 1-3 s delay relative to the moment the air stream (gust) speed begins to increase.

Table 4. Specifications of the dual-rotor wind turbine

No.	Turbine parameters	Wind turbine
1	Rated wind speed (m·s⁻¹)	12.5
2	Maximum wind speed (m·s⁻¹)	35
3	Minimum wind speed (m·s⁻¹)	2.5
4	Rotor diameter (m)	0.75/0.75
5	Number of rotor blades (pcs.)	3/3
	Generator	
6	Generator Type	Synchronous
7	Excitation	Self-excited with permanent magnets
8	Voltage supply	Brush
9	Maximum electrical power (W)	400
10	Rated electrical power (W)	300
11	Voltage [V]	12
12	Voltage control system	built-in
13	Output voltage	AC
14	Stator diameter (m) ext./int.	0.15/0.092
15	Width of the stator (m)	0.055
16	Rotor diameter (m)	0.09
17	Rotor width (m)	0.02

The wind turbine, as previously mentioned, worked under varying wind conditions and was situated on a platform 10 meters above the ground. A record of the changes in power capacity for the period
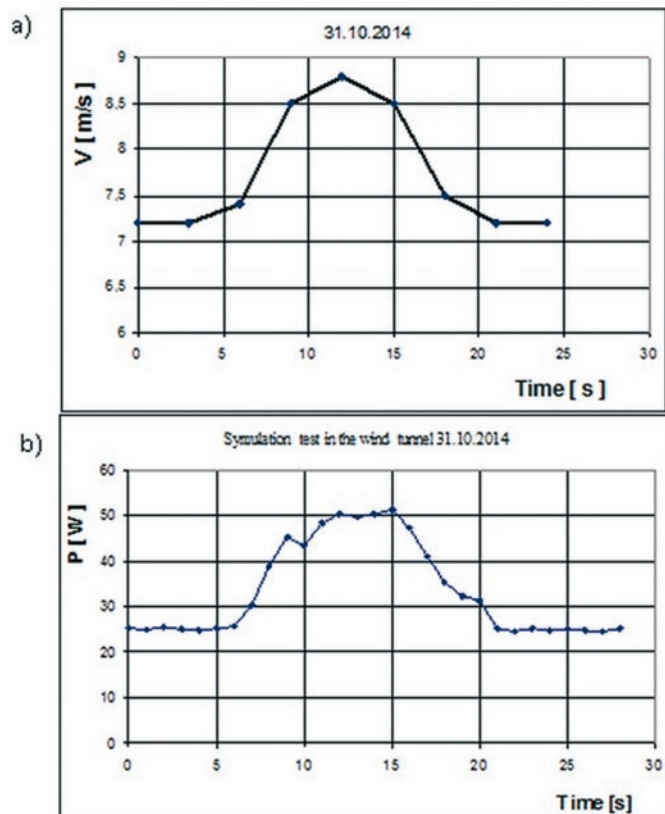

Fig. 17. Simulation of the performance of the wind turbine in the wind tunnel: a- air stream speed curve, b- generated power curve

5-6 November 2014 is given in Figure 18. In this period, approx. 12 distinct wind gusts shown in the Figure as peaks were recorded. A detailed record of the increase in the power delivered by the turbine generator during a gust of 23:36 hours, on 5 November 2014, is shown in Figure 19. In the analysed case, there was a problem concerning the recording as power was recorded at 1 s intervals while speed could only be recorded at 3 s intervals. Observations made during the wind tunnel tests were consistent with those from field studies, as the power increase followed an upward trend in wind speed and was delayed by 1-2 seconds. Registered wind speed of a 15-second gust was 9 m·s⁻¹. It should be presumed that the actual speed was slightly higher, since the value of 9 m·s⁻¹ is the average for 3 seconds, which should also explain the fact that the maximum of the power generated occurred a second earlier than the recorded maximum gust speed. During the field performance tests, wind speed rarely exceeded 7 m·s⁻¹ and the average calculated for the examined period was 2.21 m·s⁻¹ (Fig. 20). Its direction and repeatability is illustrated in Figure 21 featuring the wind rose. In accordance with the prevailing tendency in Lower Silesia these were mainly winds from the west or from its north-western
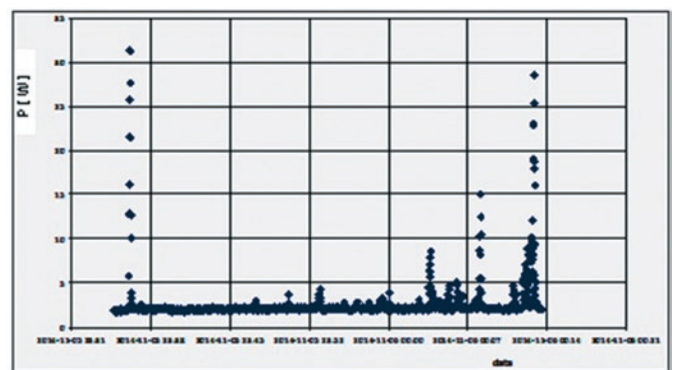

Fig. 18. Distribution of power generated by the dual-rotor wind turbine in the period: 5-6 November 2014
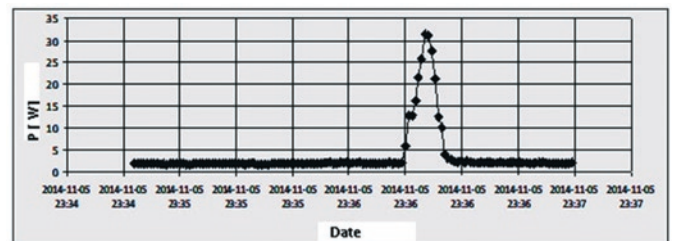

Fig. 19. Distribution of power generated by the dual-rotor wind turbine on 5 November 2014
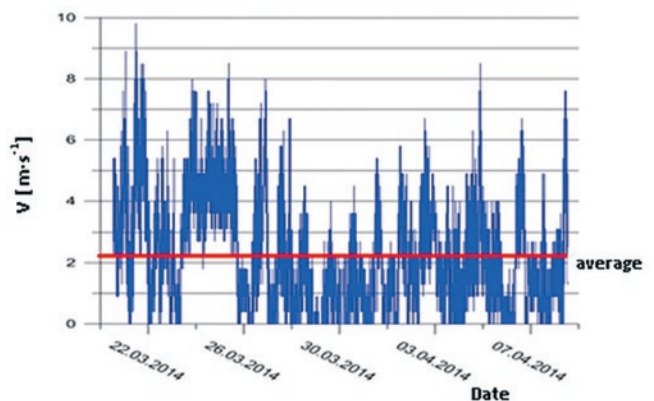

Fig. 20. Distribution of wind speed in the area where the wind turbine operated
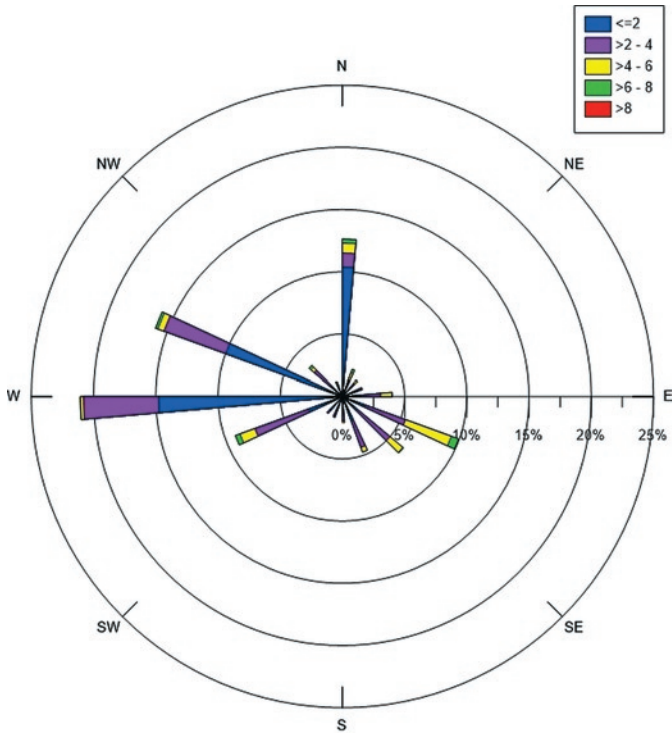
Fig. 21. Wind rose of the area of operation of the wind turbine

area. Over 80% of these winds was blowing at a speed of less than 4 m·s⁻¹.

Electrical current delivered by the wind turbine very rarely exceeded the value of 1 A, and the average for the whole testing period was 50 mA, which of course affected the value of delivered power the average of which was 0.6 W. Distribution of power generated by the wind turbine is shown in Figure 22. It has been calculated that for an average wind speed of 2.21 m·s⁻¹, the power of the wind working against the rotor of a wind turbine is approx. 6.6 W. In such poor wind conditions, the conversion efficiency of wind energy into electrical energy was only 9%.

Figures 23 and 24 show examples of the results of tests carried out in October 2014. When analysing the data from these graphs, one can observe the correlation between wind speed and power generated by the plant. For example, until 13.30 hours wind speed was increasing,
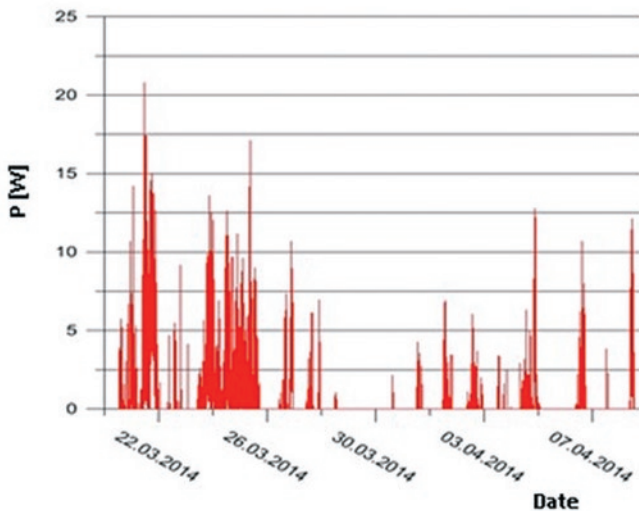

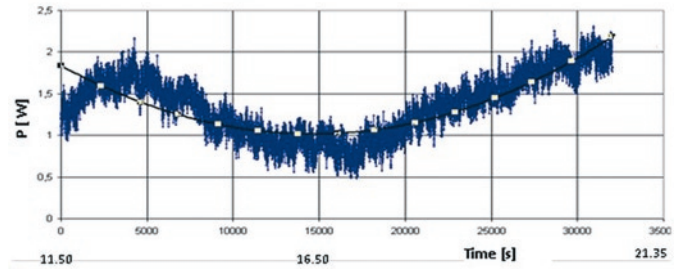*Fig. 22.   Distribution of power generated by the dual-rotor wind turbine*

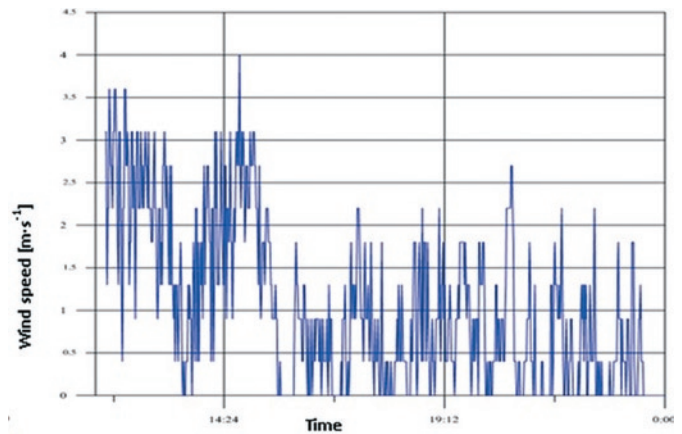*Fig. 23. Distribution of power delivered by the wind turbine on 29 October 2014*

Fig. 24. Distribution of wind speed in the area where the wind turbine operated on 29 October 2014

which resulted in a increase in power generated, while after 14.30 with decreasing wind speed the lowest power generated on that day was recorded. In the period when speed was increasing, the average power of the wind was 4.3 W (the maximum absolute error of measurement 1,17W); compared to the registered electrical power generated, it would mean that the conversion efficiency of the turbine was 36%, which appears to be a fairly optimistic result.

4. Conclusions

1. The erected open circuit wind tunnel was characterized by the coefficient of uneven air stream distribution of 1.7% at the rated speed, while the index of turbulence intensity in the entire measurement range was between 1.2 and 1.8%.
2. The NACA-type rotor blades designed for the model of a mini wind turbine increased power generated by the tested plant by 33%.
3. Statistical analysis showed that the power of the dual-rotor mini wind turbine substantially depended (at a significance level of 0.05) on air stream speed and incidence angles of the rotor blades while it did not depend on the distance between the rotors. Effect of other factors was not determined.
4. During gusts of wind, power generated by the wind turbine increased at a 1-3 s delay relative to the recorded increase in wind speed.

References

1. Arżanikow N S, Malcew W N. Aerodynamika. Warszawa: PWN, 1959.
2. Bak Ch, Fuglsang P, Johansen J, Antoniou I. Wind Tunnel Tests of the NACA 63-415 and a Modified NACA 63-415 Airfoil, Risø-R-1193(EN). 2000.
3. Capuzzi M, Pirrera A, Weaver PM. Structural design of a novel aeroelastically tailored wind turbine blade. Thin-Walled Structures 2015; 95: 7-15, http://dx.doi.org/10.1016/j.tws.2015.06.006.
4. Chong TP, Joseph PF, Davies POAL. Design and performance of an open jet wind tunnel for aero-acoustic measurement. Applied Acoustics 2009; 70: 605-614, http://dx.doi.org/10.1016/j.apacoust.2008.06.011.
5. Flaga A. Inżynieria wiatrowa. Warszawa: Wydawnictwo Arkady, 2008.
6. Goliński J A, Troskolański A T. Strumienice: teoria i konstrukcja. Warszawa: WNT, 1979.
7. Gumuła S, Knap T, Strzelczyk P, Szczerba Z. Energetyka wiatrowa. Kraków: Wyd. AGH, 2006.
8. Gumuła S, Mikoś M, Pytel K, Stępniewski Ł. Kształtowanie pola prędkości strumienia powietrza wypływającego z wentylatora osiowego. Mechanika/AGH 1999; 18(4): 499-507.
9. Gumuła S, Pytel K. Kształtowanie parametrów strugi powietrza za wentylatorem osiowym w kanale kwadratowym i w przestrzeni otwartej za kanałem. Mechanics 2005; 24(5): 246-251.
10. Hossein H, Liang C, Haitao Z, Vassilios K, Cem S, Tat-Hean G. A dual de-icing system for wind turbine blades combining high-power ultrasonic guided waves and low-frequency forced vibrations. Renewable Energy 2015; 83: 859-870, http://dx.doi.org/10.1016/j.renene.2015.05.025.
11. Idelchik I E. Handbook of Hydraulic Resistance. Jaico Publishing House 2005.
12. Jagodziński W. Silniki wiatrowe. Warszawa: PWT, 1959.
13. Karolewski B, Ligocki P. Rodzaje prądnic tarczowych. Wiad. Elektrotechniczne 2008: 8.
14. Karolewski B. Parametry modeli bezrdzeniowych prądnic tarczowych. Elektro.inf. 2011: 6.
15. Komarnicki P, Romański L, Bieniek J, Dębowski M, Pałka K. Wpływ regulacji pracy wentylatorów na równomierność rozkładu strumienia powietrza w tunelu aerodynamicznym. Inżynieria Rolnicza 2013; 2(143): 155-165.
16. Lee S, Son E, Lee S. Velocity interference in the rear rotor of a counter-rotating wind turbine. Renewable Energy 2013: 54: 235-240, http://dx.doi.org/10.1016/j.renene.2012.08.003.
17. Miąskowski W, Nalepa K, Pietkiewicz P, Komar W. Dwuwirnikowa mikrosiłownia wiatrowa z osią poziomą. Olsztyn: Wyd. UWM, 2012; 485-492.
18. Mitelet L, Oprina G, Chichaia R, Nicokaie S, Nedelcu A, Popescu M. Wind Tunnel Testing for a New Experimental Model of Counter-Rotating Wind Turbine. Procedia Engineering 2015; 100: 1141-1149, http://dx.doi.org/10.1016/j.proeng.2015.01.477.
19. Pagnini LC, Burlando M, Repetto MP. Experimental power curve of small-size wind turbines in turbulent urban environment. Applied Energy 2015; 154: 112–121, http://dx.doi.org/10.1016/j.apenergy.2015.04.117.
20. Selig M S, Guglielmo J J, Broeren A P, Giguere P. Summary of Low-Speed Airfoil Data. Virginia: SoarTech Publications, 1995; 1.
21. Seungmin L, Eunkuk S, Soogab L. Velocity interference in the rear rotor of a counter-rotating wind turbine. Renewable Energy 2013; 54: 235-240. http://dx.doi.org/10.1016/j.renene.2012.08.003
22. Seungmin L, Hogeon K, Soogab L. Analysis of aerodynamic characteristics on a counter-rotating wind turbine. Current Applied Physics 2010; 10: 1567-1739.
23. Somers D M. S822 and S823 Airfoils. October 1992--December 1993. NREL Report No. SR-500-36342, 2005; 37.
24. Sung Nam J, Tae-Soo N, Ki-Wahn R. Aerodynamic performance prediction of a 30kW counter-rotating wind turbine system. Renewable Energy 2005; 30: 631-644, http://dx.doi.org/10.1016/j.renene.2004.07.005.
25. Świtoński E, Jureczko M, Mężyk A. Optymalne projektowanie kompozytowych łopat elektrowni wiatrowej. Acta Mechanica et Automatica 2007; 1.1(1).
26. Wei X, Pan Z, Liping L. A novel folding blade of wind turbine rotor for effective power control. Energy Conversion and Management 2015; 101: 52-65, http://dx.doi.org/10.1016/j.enconman.2015.05.037.

Leszek ROMAŃSKI
Jerzy BIENIEK
Piotr KOMARNICKI
Institute of Agricultural Engineering
Wrocław University of Environmental and Life Sciences
ul. Chełmońskiego 37a, 61-530 Wrocław, Poland

E-mails: leszek.romanski@up.wroc.pl,
jerzy.bieniek@up.wroc.pl, piotr.komarnicki@up.wroc.pl

Marcin DĘBOWSKI
Faculty of Mechanical and Power Engineering
Wrocław University of Technology
ul. Wybrzeże Wyspiańskiego 27, 50-370 Wrocław, Poland

Jerzy DETYNA
Department of Mechanics, Materials Science and Engineering
Wroclaw University of Technology
ul. Smoluchowskiego 25, 50-370 Wroclaw, Poland

Emails: marcin.debowski@pwr.edu.pl,
jerzy.detyna@pwr.edu.pl